
This is an electronic reprint of the original article.
This reprint may differ from the original in pagination and typographic detail.

Lister, M. L.; Aller, M. F.; Aller, H. D.; Hodge, M. A.; Homan, D. C.; Kovalev, Y. Y.; Pushkarev, A. B.; Savolainen, T.

MOJAVE. XV. VLBA 15 GHz Total Intensity and Polarization Maps of 437 Parsec-scale AGN Jets from 1996 to 2017

Published in:
Astrophysical Journal, Supplement Series

DOI:
[10.3847/1538-4365/aa9c44](https://doi.org/10.3847/1538-4365/aa9c44)

Published: 01/01/2018







Document Version
Publisher's PDF, also known as Version of record

Please cite the original version:
Lister, M. L., Aller, M. F., Aller, H. D., Hodge, M. A., Homan, D. C., Kovalev, Y. Y., Pushkarev, A. B., & Savolainen, T. (2018). MOJAVE. XV. VLBA 15 GHz Total Intensity and Polarization Maps of 437 Parsec-scale AGN Jets from 1996 to 2017. *Astrophysical Journal, Supplement Series*, 234(1), [12].
<https://doi.org/10.3847/1538-4365/aa9c44>

This material is protected by copyright and other intellectual property rights, and duplication or sale of all or part of any of the repository collections is not permitted, except that material may be duplicated by you for your research use or educational purposes in electronic or print form. You must obtain permission for any other use. Electronic or print copies may not be offered, whether for sale or otherwise to anyone who is not an authorised user.



MOJAVE. XV. VLBA 15 GHz Total Intensity and Polarization Maps of 437 Parsec-scale AGN Jets from 1996 to 2017

M. L. Lister¹ , M. F. Aller² , H. D. Aller² , M. A. Hodge¹, D. C. Homan³ , Y. Y. Kovalev^{4,5,6} , A. B. Pushkarev^{4,7}, and T. Savolainen^{5,8,9} 

¹ Department of Physics and Astronomy, Purdue University, 525 Northwestern Avenue, West Lafayette, IN 47907, USA

² Department of Astronomy, University of Michigan, 311 West Hall, 1085 S. University Avenue, Ann Arbor, MI 48109, USA

³ Department of Physics, Denison University, Granville, OH 43023, USA

⁴ Astro Space Center of Lebedev Physical Institute, Profsoyuznaya 84/32, 117997 Moscow, Russia

⁵ Max-Planck-Institut für Radioastronomie, Auf dem Hügel 69, D-53121 Bonn, Germany

⁶ Moscow Institute of Physics and Technology, Dolgoprudny, Institutsky per. 9, Moscow region, 141700, Russia

⁷ Crimean Astrophysical Observatory, 98409 Nauchny, Crimea, Russia

⁸ Aalto University Department of Electronics and Nanoengineering, PL 15500, FI-00076 Aalto, Finland

⁹ Aalto University Metsähovi Radio Observatory, Metsähovintie 114, FI-02540 Kylmälä, Finland

Received 2017 September 18; revised 2017 November 7; accepted 2017 November 15; published 2018 January 15

Abstract

We present 5321 mas-resolution total intensity and linear polarization maps of 437 active galactic nuclei (AGNs) obtained with the VLBA at 15 GHz as part of the MOJAVE survey, and also from the NRAO data archive. The former is a long-term program to study the structure and evolution of powerful parsec-scale outflows associated with AGNs. The targeted AGNs are drawn from several flux-limited radio and γ -ray samples, and all have correlated VLBA flux densities greater than ~ 50 mJy at 15 GHz. Approximately 80% of these AGNs are associated with γ -ray sources detected by the *Fermi* LAT instrument. The vast majority were observed with the VLBA on 5–15 occasions between 1996 January 19 and 2016 December 26, at intervals ranging from a month to several years, with the most typical sampling interval being six months. A detailed analysis of the linear and circular polarization evolutions of these AGN jets is presented in the other papers in this series.

Key words: BL Lacertae objects: general – galaxies: active – galaxies: jets – quasars: general – radio continuum: galaxies

Supporting material: animation, figure set, machine-readable table

1. Introduction

The collimated outflows from powerful active galactic nuclei (AGNs) represent some of the most long-lived and energetic processes ever discovered, and are now recognized to have played a prominent role in the early structure formation of our universe via feedback mechanisms (e.g., Fabian 2012; Heckman & Best 2014). Due to their exceedingly compact synchrotron radio emission, AGN jets have long been a primary target of very long baseline interferometry (VLBI) observations, which provide sub-milliarcsecond resolution maps on scales out to several hundred parsecs from the central engine. With the construction of the world’s first dedicated multi-element VLBI system, the Very Long Baseline Array (VLBA) in 1994, it became possible to study large numbers of jets with full polarimetry at regular intervals. The structure and evolution of linearly and circularly polarized jet emission provides crucial data for understanding many poorly understood aspects of the flows, including their collimation mechanisms, instability modes, magnetic field structure, and the nature of the plasma itself (see, e.g., Wardle 2013; Agudo 2015). In 2002 we began a follow-up program to the 2 cm VLBA survey of Kellermann et al. (1998), named MOJAVE (Monitoring of Jets in AGNs with VLBA Experiments) with the goal of studying the parsec-scale evolution of a large, complete sample of AGN jets with full polarization VLBA imaging. The MOJAVE sample was subsequently expanded to encompass an additional set of AGN jets detected in γ -rays by the *Fermi* LAT instrument, and other compact radio-loud AGNs of interest to the community. More details on

individual objects and their total intensity evolution can be found in other papers in this series (e.g., Lister et al. 2013, 2016).

In this paper we present multi-epoch 15 GHz VLBA total intensity and linear polarization maps of 437 AGNs observed between 1996 January 19 and 2016 December 26, primarily as part of the MOJAVE program, with supplementary data obtained from the NRAO archive. In Lister & Homan (2005) we discussed the first epoch linear polarization maps of the original MOJAVE flux-density limited AGN sample, and we described their circular polarization properties in Homan & Lister (2006). We will present a full multi-epoch analysis of the linear and circular polarization characteristics of our extended sample of 437 AGNs in future papers.

2. Observational Data

2.1. Sample Selection

The VLBA maps in this paper are of 437 compact, radio-loud AGNs observed as part of the MOJAVE program. The latter originally started as a complete set of 135 AGNs with J2000 declination $> -20^\circ$ and galactic latitude, $|b| > 2^\circ 5'$ whose 15 GHz VLBA flux density exceeded 1.5 Jy (≥ 2 Jy for sources below the celestial equator) at any epoch between 1994.0 and 2004.0 (Lister et al. 2009a). This radio-selected sample was later expanded to encompass all 181 AGNs above a declination of -30° that were known to have exceeded 1.5 Jy in VLBA 15 GHz flux density at any epoch between 1994.0 and 2010.0 (Lister et al. 2013).

With the launch of the *Fermi* observatory in 2008, two new γ -ray-based AGN samples were added to MOJAVE. The 1FM sample (Lister et al. 2011) consists of all 116 AGNs in the 1FGL catalog (Abdo et al. 2010) above a declination of -30° and galactic latitude of $|b| > 10^\circ$, with average integrated *Fermi* LAT >0.1 GeV energy flux above 3×10^{-11} erg cm $^{-2}$ s $^{-1}$. In 2013, a new hard spectrum MOJAVE sample of 132 AGNs was added, which had a declination of $>-20^\circ$, a total 15 GHz VLBA flux density of >0.1 Jy, and a mean *Fermi* 2LAC (Ackermann et al. 2011) or 3LAC catalog (Ackermann et al. 2015) spectral index harder than 2.1.

Of the 437 AGNs presented in this paper, 319 are members of one or more of the above samples. An additional 105 AGNs are members of either the precursor survey to MOJAVE (the 2 cm VLBA survey; Kellermann et al. 1998), the low-luminosity MOJAVE AGN sample (Lister et al. 2013), the 3rd EGRET γ -ray catalog (Hartman et al. 1999), the 3FGL *Fermi* LAT γ -ray catalog (Acerro et al. 2015), or the ROBOPOL optical polarization monitoring sample (Pavlidou et al. 2014). Finally, we have included 13 AGNs that were originally candidates for the above samples, but did not meet the final selection criteria.

A summary of the sample in terms of optical classification and γ -ray emission can be found in Table 1. The common feature of these AGNs is that they all have bright, compact radio emission on milliarcsecond scales ($\gtrsim 50$ mJy at 15 GHz). Since such emission is usually associated with relativistically beamed jets, the sample is primarily composed of flat-spectrum radio quasars (61%) and BL Lac objects (29%), which have powerful jets oriented at small angles to the line of sight (i.e., blazars). A total of 27 radio galaxies have made it into the sample due to their low redshift, or as a result of having GHz-peaked radio spectra. Additionally, there are 5 narrow-line Seyfert 1 galaxies, and 14 AGNs that lack identified optical counterparts. A large fraction of the sample (80%) is associated with 0.1–100 GeV γ -ray detections made by the *Fermi* LAT instrument, and 35 AGNs are listed as known TeV γ -ray emitters in TEVCAT.¹⁰

2.2. VLBA Observations

The data consist of 5321 observations of 437 AGNs in the 15 GHz band, obtained between 1996 January 19 and 2016 December 26 with the VLBA in full polarization mode (Table 2). All targets were bright enough for direct interferometric fringe detection with 2048 Mbps VLBA observations at 15 GHz (i.e., $\gtrsim 50$ mJy) during at least one epoch. In the case of two partially resolved AGNs (TXS 0831+557 and TXS 0954+556), no interferometric fringes were found at any epoch on the longest (Maunakea and St. Croix) baselines during data-processing.

Most of the VLBA observations (86%) were carried out as part of the MOJAVE program (Lister et al. 2009a), while the remainder were downloaded from the NRAO archive¹¹ and processed for the purpose of increasing the number of epochs on particular AGNs. Our minimal criteria for the individual observations were: (i) at least 8 of 10 VLBA antennas present, (ii) either the Maunakea or the St. Croix antenna present for some portion of the observation, (iii) a minimum of three scans reasonably separated over a range of hour angle, (iv) available

Table 1
AGN Sample Properties

Optical Class (1)	<i>Fermi</i> γ -ray (2)	TeV γ -ray (3)	Total (4)
Quasar	203	5	265
BL Lac	121	28	127
Radio Galaxy	10	2	27
Narrow Line Sy 1	5	0	5
Unidentified	12	0	13
Total	351	35	437

Note. The columns are as follows: (1) optical classification, (2) known associations with a *Fermi* LAT γ -ray source, (3) TeV γ -ray sources in TEVCAT, (4) total number of sources.

scans on suitable electric vector position angle and instrumental polarization (feed leakage) calibrators during the observing session.

Most of the AGNs have between 5 and 15 VLBA observation epochs, although a substantial number have considerably more epochs (up to 128, for BL Lac = TXS 2200+420), and 32 AGNs have 4 epochs or fewer (Figure 1). The median time interval between observations varies from 35 days for BL Lac to roughly 2 years for TXS 2021+614 and PKS B1345+125 (Figure 2). This large range reflects the observational strategy of the MOJAVE program, which aims to observe each AGN jet with a cadence appropriate for its angular expansion speed (Lister et al. 2016).

We calibrated and edited the data in AIPS using the standard techniques described in the AIPS Cookbook, and exported them to the DIFMAP package (Shepherd 1997) for imaging. A full description of the method can be found in Lister et al. (2009a). We determined the amplitudes and phases of the complex feed leakage terms for each IF and antenna by taking the median of the solutions obtained from the AIPS task LPCAL on bright, core-dominated AGNs that were either unpolarized or had relatively simple polarization structures. For the majority of observations obtained prior to 2013 September 1, we determined the instrumental electric vector position angle (EVPA = $(1/2) \arctan(U/Q)$, where Q and U are Stokes parameters) rotation using several leakage term phases that were constant over time at certain antennas (see, e.g., Gomez et al. 2002). This method requires an external calibration to establish the absolute EVPA directions on the sky; for this purpose we used near-simultaneous single-dish measurements of selected core-dominated jets at 14.5 GHz made at the University of Michigan Radio Observatory, up until its closure in 2012 July. With the introduction of new digital electronics at the VLBA antennas in mid-2013, the leakage term phases became unstable over time. For observations after this date we therefore relied on optically thin jet features in multiple AGNs that we have found to have relatively stable EVPAs for calibration purposes. We also used this method for several NRAO archive observations that used a different recording setup from our regular MOJAVE observations, and thus had different leakage term phases. Based on our comparisons of highly compact AGNs to near-simultaneous single-dish observations, we estimate our VLBA EVPA measurements are accurate to $\sim 5^\circ$, and our flux densities are accurate to $\sim 5\%$.

¹⁰ <http://tevcat.uchicago.edu>

¹¹ <http://archive.nrao.edu>

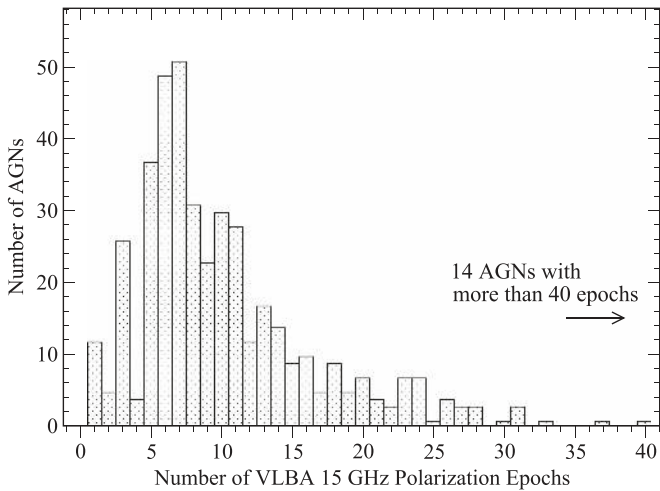


Figure 1. Distribution of the number of 15 GHz VLBA polarization observations for 437 AGNs in the MOJAVE program.

2.3. Map Characteristics

We measured the rms noise levels (σ) in the Stokes I , Q , and U maps by shifting the map center by 1 arcsec and calculating the standard deviation of the (blank sky) pixel intensity distribution. The Q and U maps typically had similar noise characteristics, so we will hereafter refer to $\sigma_{Q,U}$ as the average of these two noise levels. Our large set of maps has a factor of ~ 5 range of rms map noise level, due to differences in the total integration time, number of scans and antennas present in each observing session, and in the observed bandwidth (as set by the maximum recordable bit rate). The latter has steadily increased over time, due to hardware upgrades at the VLBA antennas. This is apparent in Figure 3, where we plot the median $\sigma_{Q,U}$ of the maps from each observing session having more than four AGNs versus the date of observation. The most recent MOJAVE observations, recorded at 2048 Mbps with 2-bit sampling for a total observing bandwidth of 256 MHz per polarization, have typical map rms noise levels of 0.1 mJy beam $^{-1}$ in Stokes I , Q and U . This represents a factor of ~ 3 improvement since the start of the MOJAVE VLBA program in 2002.

As discussed by Wardle & Kronberg (1974) and Simmons & Stewart (1985), the noise statistics of a linear polarization map ($P = \sqrt{Q^2 + U^2}$) are Ricean, since it is a vector addition of the Q and U maps, each of which have Gaussian noise statistics. In the case of a blank sky region, or one with a low polarization signal-to-noise ratio, the noise statistics of the P map approximately follow a Rayleigh distribution, which has a mean $(\pi/2)^{1/2}\sigma_{Q,U}$ and variance $(2 - \pi/2)\sigma_{Q,U}^2$. It is only in high signal-to-noise regions ($\gtrsim 3$) that the P map noise statistics approach a Gaussian distribution, with variance $\sigma_{Q,U}^2$. The corresponding noise in the fractional polarization map will be $\sigma_m = \sigma_{Q,U}/I$ (see, e.g., Appendix B of Hovatta et al. 2012).

Additional complications arise with polarization imaging due to errors associated with the antenna feed leakage terms (Roberts et al. 1994), and errors during the CLEAN process due to incomplete (u, v) plane coverage (Hovatta et al. 2012). Imperfect correction of the leakage of polarization signal orthogonal to the nominal polarization causes polarized emission to be spread throughout the map in a non-uniform manner. Since these errors are proportional to the total Stokes I intensity, they can be

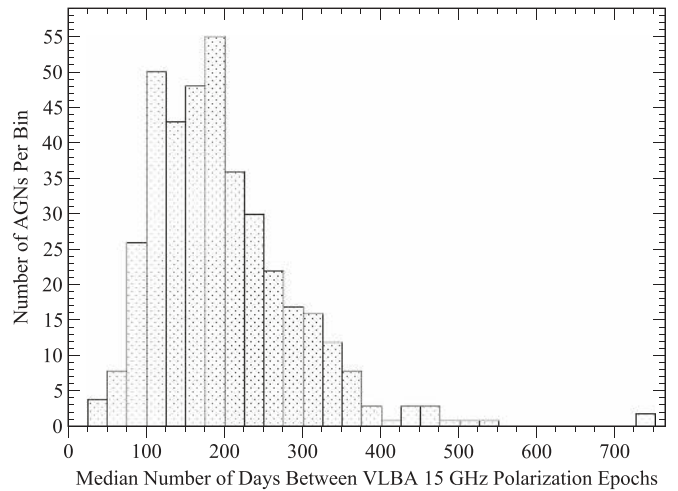


Figure 2. Distribution of the median interval between 15 GHz VLBA polarization observations for 437 AGNs in the MOJAVE program.

significant in maps of bright radio sources. This frequently leads to spurious high fractional polarization values ($\gtrsim 40\%$) at the edges of the jets in our maps, where the total intensity falls off exponentially. These regions of the polarization maps should therefore be interpreted with caution.

2.4. Contour Maps

In Figure 4, we present “dual-plot” maps of each VLBA AGN observation at all available epochs. We previously published first-epoch maps of this type for the original MOJAVE sample in Lister & Homan (2005). The FWHM dimensions and orientation of the naturally weighted elliptical Gaussian restoring beam are indicated by a cross in the lower left corner of each map. The beam size varies somewhat with the declination of the AGN and number of antennas, but has typical dimensions of 1.1 mas \times 0.5 mas. We gridded each of the Stokes maps with a scale of 0.1 mas per pixel. We list the parameters of the restoring beam, base contour levels, total cleaned flux densities, and blank sky map noise levels for each map in Table 2. The false color corresponds to fractional polarization, and is superimposed on a total intensity contour map of the radio emission. The false-color scale is truncated at a fractional polarization level of 50%, since such high values are generally not seen at the same locations in successive epochs on a given jet, and are most likely spurious. We also plot no fractional polarization in regions that lie below the lowest total intensity contour. The latter typically corresponds to three times the rms noise level of the map, although this can be higher in the cases of AGNs with poorer interferometric coverage (due to very low or near-equatorial declination) or very bright jet cores (due to dynamic range limitations on the map). Similarly, the lowest polarization contour is typically 3 times $\sigma_{Q,U}$, but in $\sim 15\%$ of the epochs it is > 5 times $\sigma_{Q,U}$, due to a high peak total intensity in the map, or polarization feed leakage errors. We have not made any Ricean de-biasing corrections (i.e., $P_{\text{corr}} = P_{\text{obs}} \sqrt{1 - (\sigma_P/P_{\text{obs}}^2)}$) to the maps, since these are $\lesssim 5\%$ for regions above our lowest polarization contour level.

Since any absolute sky positional information is lost due to self-calibration, the map origin is placed at the total intensity

Table 2
Summary of 15 GHz Image Parameters

Source	Alias	Epoch	B_{maj} (mas)	B_{min} (mas)	B_{pa} ($^{\circ}$)	I_{tot} (mJy)	σ_I (mJy beam $^{-1}$)	I_{base} (mJy beam $^{-1}$)	P_{tot} (mJy)	$\sigma_{Q,U}$ (mJy beam $^{-1}$)	P_{base} (mJy beam $^{-1}$)	EVPA ($^{\circ}$)	Fig. Num.
(1)	(2)	(3)	(4)	(5)	(6)	(7)	(8)	(9)	(10)	(11)	(12)	(13)	(14)
0003+380	S4 0003+38	2006 Mar 9	1.01	0.73	18	650	0.44	1.15	16	0.45	1.48	78	4.1
		2006 Dec 1	0.85	0.58	-17	512	0.41	1.10	9.2	0.46	1.42	146	4.2
		2007 Mar 28	0.86	0.61	-15	604	0.33	0.80	5.6	0.35	1.08	144	4.3
		2007 Aug 24	0.92	0.58	-28	555	0.25	0.80	7.3	0.30	0.88	166	4.4
		2008 May 1	0.82	0.57	-9	808	0.24	0.70	12	0.26	0.84	178	4.5
		2008 Jul 17	0.84	0.55	-12	727	0.22	0.60	17	0.25	0.79	175	4.6
		2009 Mar 25	0.84	0.62	-12	435	0.16	0.50	10	0.17	0.56	145	4.7
		2010 Jul 12	0.89	0.54	-12	438	0.17	0.50	10	0.19	0.63	132	4.8
		2011 Jun 6	0.91	0.54	-10	605	0.18	0.50	2.1	0.20	0.63	108	4.9
0003-066	NRAO 005	2013 Aug 12	0.84	0.53	-4	668	0.20	0.50	9.8	0.21	0.75	139	4.10
		2003 Feb 5	1.32	0.53	-6	2842	0.31	1.40	103	0.37	1.00	17	4.11
		2004 Jun 11	1.30	0.49	-7	3273	0.32	1.40	255	0.61	1.57	22	4.12
		2005 Mar 23	1.32	0.53	-5	3034	0.27	1.50	129	0.32	1.38	4	4.13
		2005 Jun 3	1.37	0.53	-8	3017	0.23	1.40	110	0.30	1.00	175	4.14

Notes. The columns are as follows: (1) B1950 name, (2) other name, (3) date of VLBA observation, (4) FWHM major axis of the restoring beam (milliarcseconds), (5) FWHM minor axis of restoring beam (milliarcseconds), (6) position angle of the major axis of the restoring beam (degrees), (7) total cleaned I flux density (mJy), (8) rms noise level of the Stokes I image (mJy per beam), (9) lowest I contour level (mJy per beam), (10) total cleaned P flux density (mJy), or upper limit, based on 3 times the P rms noise level, (11) average of the blank sky rms noise level in Stokes Q and U images (mJy per beam), (12) lowest linear polarization contour level (mJy per beam), (13) integrated electric vector position angle (degrees), (14) online Figure 4 element number.

^a NRAO archive epoch.

(This table is available in its entirety in machine-readable form.)

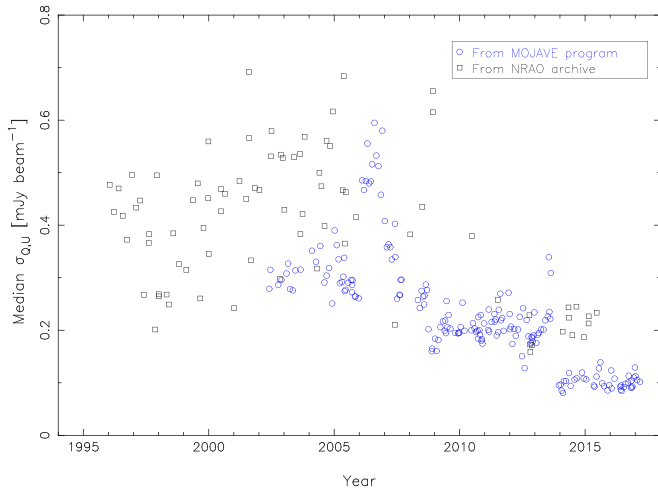


Figure 3. Plot of median Stokes Q , U blank-sky rms noise levels for individual observing sessions from the MOJAVE program (blue circles) and the NRAO archive (black crosses). The increased noise in MOJAVE maps in 2006–2007 is due to the addition of other VLBA observing frequencies during that period (see Hovatta et al. 2012).

Gaussian model-fit position of the core feature, as described by Lister et al. (2016). The latter is typically the brightest feature in the map, located at the optically thick surface close to the base of the jet. The positional accuracy of the core model-fit is typically 20% of the FWHM beam dimension listed in Table 2, as discussed in Lister et al. (2009b).

A second map of the jet emission is located at an arbitrary positional offset from the first, and consists of polarized intensity contours, and the lowest total intensity contour for reference. The overlaid sticks indicate the observed electric

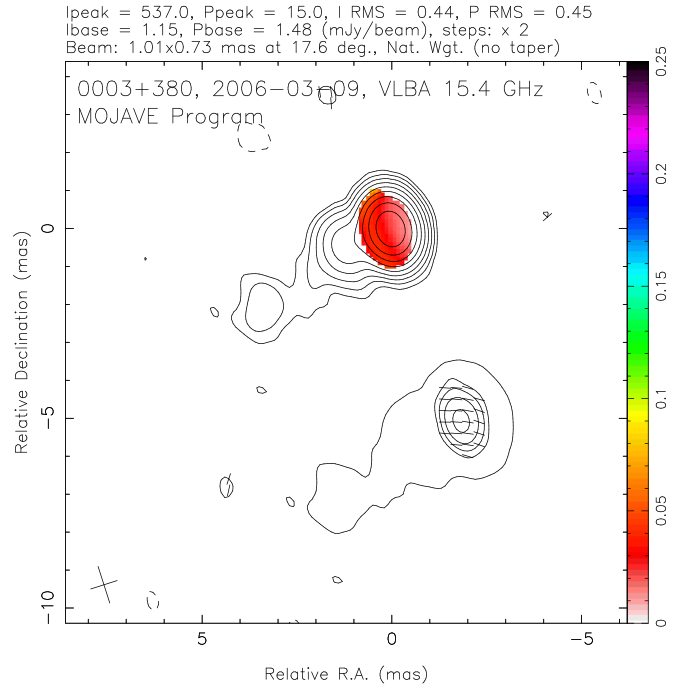


Figure 4. 15 GHz VLBA maps of the MOJAVE AGN sample. Each panel contains two contour maps of the radio source, the first consisting of I contours in successive integer powers of two times the lowest contour level, with linear fractional polarization overlaid according to the color wedge. A single negative I contour equal to the base contour level is also plotted. The second map includes the lowest positive I contour from the first map, and linearly polarized intensity contours, also in increasing powers of two. The sticks indicate the electric polarization vector directions, uncorrected for Faraday rotation. The FWHM dimensions and orientation of the elliptical Gaussian restoring beam are indicated by a cross in the lower left corner of the map.

(The complete figure set (5321 images) is available.)

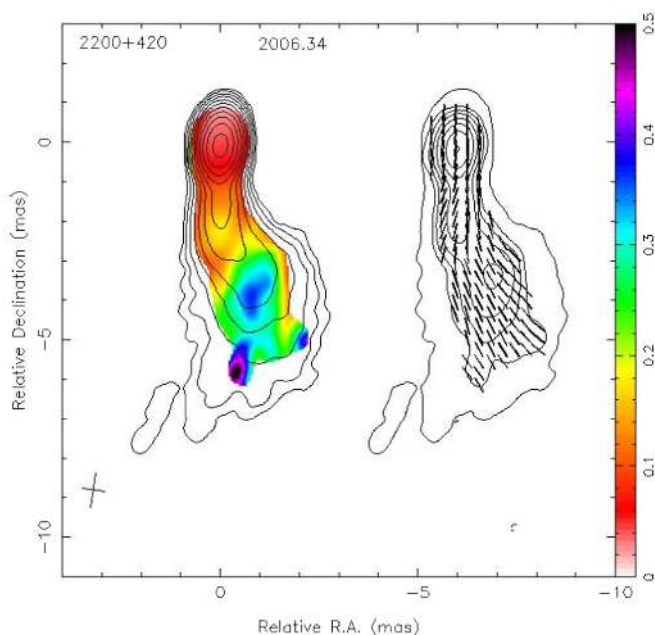


Figure 5. Linearly interpolated time-lapse movie made from the multi-epoch VLBA maps for BL Lac. Each epoch was restored with a median beam, whose FWHM dimensions ($0.87 \text{ mas} \times 0.56 \text{ mas}$ at -8.4°) are indicated by the cross in the lower left corner. The false color and contour scheme follows that use in Figure 4. The base contours in total intensity and polarization are 2 mJy per beam, and one year of calendar time corresponds to 7 s in the time-lapse movie. (An animation of this figure is available.)

vector directions, and are of an arbitrary fixed length. We have not corrected their orientations for any Faraday rotation either internal or external to the AGN jet. Our rotation measure study of the MOJAVE sample (Hovatta et al. 2012) showed that the emission from most of these jets experiences only a few degrees of Faraday rotation (typically in the region near the base of the jet) at 15 GHz . The total intensity and polarization contours are plotted at increasing powers of two times the base contour level listed on the map and in Table 2.

3. Time-lapse Movies

In Figure 5 we show a time-lapse MPEG movie of the multi-epoch VLBA polarization and total intensity maps for BL Lac from 1999 May 16 to 2016 December 26. Movies for other AGNs can be found on the MOJAVE web site.¹² We constructed the movie using a two-point linear interpolation across each successive epoch, treating each map pixel independently. One year of calendar time corresponds to 7 s in the time-lapse. Prior to interpolation, we registered all of the epoch maps to the Gaussian-fit core positions and restored them to a scale of 0.05 ms per pixel using identical median beam dimensions ($0.87 \text{ mas} \times 0.56 \text{ mas}$ at -8.4°) that were based on the full set of naturally weighted VLBA epochs available for this AGN. The individual frames of the movie follow the same format as the individual epoch maps of Figure 4; however, the base contours in total intensity and polarization are set to 2 mJy per beam in all of the movie frames.

4. Summary

We have presented 5321 mas -resolution, VLBA 15 GHz total intensity and linear polarization maps of 437 AGN jets obtained between 1996 January 19 and 2016 December 26 as part of the MOJAVE program, and also from the NRAO data archive. These AGNs are drawn from several flux-limited radio and γ -ray samples, and are all compact, with correlated flux densities greater than $\sim 50 \text{ mJy}$. Most were observed on at least 5–15 occasions between 1996 and 2017, at intervals ranging from a month to several years, with the most typical interval being 6 months. We have analyzed the multi-epoch total intensity evolution of most of these jets in a series of papers (Homan et al. 2009; Lister et al. 2009b, 2013; Homan et al. 2015), with the most recent analysis presented by Lister et al. (2016). We will present a detailed analysis of the linear and circular polarization evolutions of these AGN jets in upcoming papers in this series.

The MOJAVE project was supported by NASA-*Fermi* grants NNX08AV67G, NNX12A087G, and NNX15AU76G. M.F.A. was supported in part by NASA-*Fermi* GI grants NNX09AU16G, NNX10AP16G, NNX11AO13G, NNX13AP18G, and NSF grant AST-0607523. Y.Y.K. and A.B.P. were supported by the Russian Foundation for Basic Research (project 17-02-00197), the Basic Research Program P-7 of the Presidium of the Russian Academy of Sciences and the government of the Russian Federation (agreement 05.Y09.21.0018). T.S. was supported by the Academy of Finland projects 274477 and 284495. The Long Baseline Observatory and the National Radio Astronomy Observatory are facilities of the National Science Foundation operated under cooperative agreement by Associated Universities, Inc. This work made use of the Swinburne University of Technology software correlator (Deller et al. 2011), developed as part of the Australian Major National Research Facilities Programme and operated under licence.

ORCID iDs

M. L. Lister <https://orcid.org/0000-0003-1315-3412>
M. F. Aller <https://orcid.org/0000-0003-2483-2103>
H. D. Aller <https://orcid.org/0000-0003-1945-1840>
D. C. Homan <https://orcid.org/0000-0002-4431-0890>
Y. Y. Kovalev <https://orcid.org/0000-0001-9303-3263>
T. Savolainen <https://orcid.org/0000-0001-6214-1085>

References

- Abdo, A. A., Ackermann, M., Ajello, M., et al. 2010, *ApJS*, **188**, 405
Acero, F., Ackermann, M., Ajello, M., et al. 2015, *ApJS*, **218**, 23
Ackermann, M., Ajello, M., Allafort, A., et al. 2011, *ApJ*, **743**, 171
Ackermann, M., Ajello, M., Atwood, W. B., et al. 2015, *ApJ*, **810**, 14
Agudo, I. 2015, in *The Many Facets of Extragalactic Radio Surveys: Towards New Scientific Challenges*, AGN Physics (Trieste: SISSA), 72
Deller, A. T., Brisken, W. F., Phillips, C. J., et al. 2011, *PASP*, **123**, 275
Fabian, A. C. 2012, *ARA&A*, **50**, 455
Gomez, J. L., Marscher, A. P., Alberdi, A., Jorstad, S. G., & Agudo, I. 2002, VLBA Scientific Memo No. 30, (<https://science.nrao.edu/facilities/vlba/publications/memos/sci/sci30memo.ps>)
Hartman, R. C., Bertsch, D. L., Bloom, S. D., et al. 1999, *ApJS*, **123**, 79
Heckman, T. M., & Best, P. N. 2014, *ARA&A*, **52**, 589
Homan, D. C., Kadler, M., Kellermann, K. I., et al. 2009, *ApJ*, **706**, 1253
Homan, D. C., & Lister, M. L. 2006, *AJ*, **131**, 1262
Homan, D. C., Lister, M. L., Kovalev, Y. Y., et al. 2015, *ApJ*, **798**, 134
Hovatta, T., Lister, M. L., Aller, M. F., et al. 2012, *AJ*, **144**, 105

¹² <http://www.physics.purdue.edu/MOJAVE>

- Kellermann, K. I., Vermeulen, R. C., Zensus, J. A., & Cohen, M. H. 1998, *AJ*, **115**, 1295
- Lister, M. L., Aller, H. D., Aller, M. F., et al. 2009a, *AJ*, **137**, 3718
- Lister, M. L., Aller, M., Aller, H., et al. 2011, *ApJ*, **742**, 27
- Lister, M. L., Aller, M. F., Aller, H. D., et al. 2013, *AJ*, **146**, 120
- Lister, M. L., Aller, M. F., Aller, H. D., et al. 2016, *AJ*, **152**, 12
- Lister, M. L., Cohen, M. H., Homan, D. C., et al. 2009b, *AJ*, **138**, 1874
- Lister, M. L., & Homan, D. C. 2005, *AJ*, **130**, 1389
- Pavlidou, V., Angelakis, E., Myserlis, I., et al. 2014, *MNRAS*, **442**, 1693
- Roberts, D. H., Wardle, J. F. C., & Brown, L. F. 1994, *ApJ*, **427**, 718
- Shepherd, M. C. 1997, in ASP Conf. Ser. 125, *Astronomical Data Analysis Software and Systems VI*, ed. G. Hunt & H. E. Payne (San Francisco, CA: ASP), 77
- Simmons, J. F. L., & Stewart, B. G. 1985, *A&A*, **142**, 100
- Wardle, J. F. C. 2013, *EPJWC*, **61**, 06001
- Wardle, J. F. C., & Kronberg, P. P. 1974, *ApJ*, **194**, 249